AIP | Journal of Applied Physics

Efficiency of quasiparticle creation in proximized superconducting photon detectors

R. A. Hijmering, P. Verhoeve, D. D. E. Martin, A. G. Kozorezov, J. K. Wigmore et al.

Citation: J. Appl. Phys. **105**, 123906 (2009); doi: 10.1063/1.3141840
View online: http://dx.doi.org/10.1063/1.3141840
View Table of Contents: http://jap.aip.org/resource/1/JAPIAU/v105/i12
Published by the American Institute of Physics.

Efficiency of quasiparticle creation in proximized superconducting photon detectors

R. A. Hijmering,[1,a] P. Verhoeve,[1] D. D. E. Martin,[1] A. G. Kozorezov,[2] J. K. Wigmore,[2] R. Venn,[3] P. J. Groot,[4] and I. Jerjen[1]
[1]*Advanced Studies and Technology Preparation Division, Directorate of Science and Robotic Exploration of the European Space Agency, P.O. Box 299, 2200 AG Noordwijk, The Netherlands*
[2]*Department of Physics, Lancaster University, Lancaster LA1 4YB, United Kingdom*
[3]*Cambridge MicroFab Ltd., Broadway, Bourn, Cambridgeshire CB3 7TA, United Kingdom*
[4]*Department of Astrophysics, Radboud University Nijmegen, P.O. Box 9010, 6500 GL Nijmegen, The Netherlands*

(Received 27 January 2009; accepted 3 May 2009; published online 17 June 2009)

In previous work using thin superconducting films as photon detectors it has been assumed implicitly that the quasiparticle yield in proximized superconducting bilayers should be the same as for a pure superconducting layer with the same energy gap. The reasoning is that, following the energy down conversion cascade, the resultant quasiparticles will all finish up at the edge of the density of states, which has the same energy throughout the whole structure regardless or whether it is pure or proximized. In this paper we show that, although the energy gap is the same, the actual density of quasiparticle states may vary considerably across a proximized structure, with a secondary peak at the energy of the higher gap material. Our calculations indicate that this peak can give rise to the generation of excess subgap phonons through which a larger portion of the original photon energy is lost from the quasiparticle system. The associated lower quasiparticle yield effectively reduces the responsivity of the proximized detector and affects the limiting energy resolution. The predictions have been confirmed by experimental results obtained with a distributed read out imaging detector (DROID) in which the response to photons absorbed in a pure Ta layer and in a Ta/Al proximized structure could be compared directly. © *2009 American Institute of Physics*. [DOI: 10.1063/1.3141840]

I. INTRODUCTION

Due to their spectroscopic properties superconducting detectors are ideal for use as photon counting spectrophotometers.[1–3] In these detectors the energy of the absorbed photon is converted into a large quantity of quasiparticles or phonons via a down conversion process which occurs in three stages.[4–6] First the energy of the photon E_0 is released into a photoelectron which excites secondary electrons and plasmons. This stage of the down conversion process is dominated by strong electron-electron interactions. The second stage starts at a lower energy $E_1 \approx 1$ eV, when the electron-phonon interaction becomes dominant; the electrons begin to emit phonons with energy close to the Debye energy Ω_D. In the third stage the mixed distribution of phonons and quasiparticles evolves into a quasiparticle distribution at the edge of the energy gap of the superconductor. During this stage energy is lost via phonon loss into the substrate, mainly of phonons which do not have sufficient energy to break a Cooper pair and create two more quasiparticles.

Depositing one superconducting layer on top of a second superconducting layer of different material will modify the properties of both materials around the interface (the proximity effect). If the thicknesses of the layers similar to or smaller than the coherence length the properties of both materials will be modified throughout the entire bilayer. Although the density of states is broadened and will differ in the two materials, the energy gap will remain constant throughout the complete structure at a value intermediate between the energy gaps of the two individual materials determined by the relative layer thicknesses. Since after the down conversion process the quasiparticles will reside at the energy gap of the complete structure it is very often assumed that, although the devices are not BCS-type (following the theory as described by Bardeen *et al.*[7]), the down conversion will progress in the same manner and the standard relation for the number of quasiparticles created would still be valid, Eq. (1).

Quasiparticle dynamics and relaxation in superconductors are currently of great interest in numerous studies. Especially the discovery on an extra relaxation channel reducing the quasiparticle relaxation time and the likely involvement of magnetic impurities has provided a boost in this field.[8–10] In this paper we will look at the creation of quasiparticles and consider the final stage of down conversion process, where energy loss via subgap phonons is of importance, with particular reference to proximized superconducting tunnel junctions (STJs). The STJ consists of two thin layers of superconducting material separated by an insulating layer. As detectors they are sensitive for energies ranging from the near-infrared up to x rays, they can handle count rates up to tens of kilohertz and they provide each event with a submicrosecond accurate time stamp. The photon energy which is

[a]Electronic mail: rhijmeri@rssd.esa.int.

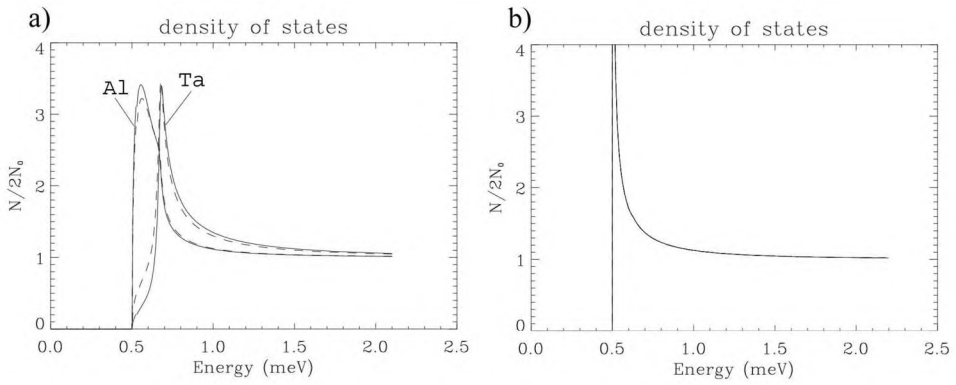

FIG. 1. (a) The quasiparticle density of states in a proximized Ta/Al bilayer with thicknesses 100/30 nm. The solid lines show the density of states in the two materials at their free interfaces and the dashed lines show the quasiparticle density of states on either side of the interface between the two materials. The energy gap Δ_{s1+s2} is equal to 500 meV and the broadened peak in the tantalum layer is at $\Delta_{s2}=\Delta_{Ta}=700$ meV. (b) The BCS counterpart density of states which only shows a singularity at the energy gap.

absorbed in the superconducting material is converted, via the down conversion process, into a large number of quasiparticles. These quasiparticles can tunnel across the thin barrier and, by applying a dc bias voltage across the junctions they can be detected as a measurable current pulse. To avoid a significant population of thermally excited quasiparticles the detector has to be cooled well below the critical temperature ($T<0.1T_c$) of the material, thereby constraining the operating temperature. For the widely used tantalum devices this operating temperature is around 400 mK. Aluminum is often used in tantalum STJs, between the tantalum layer and tunnel barrier, in order to reduce the energy gap, thus improving the charge output, and to confine ("trap") the quasiparticles near the tunnel barrier, enhancing the tunnel rate.[11]

To increase the active area position sensitive configurations, distributed read out imaging detectors (DROIDs)[12] are being developed. In general these consist of a large absorber area with STJ detectors at the edges. The quasiparticles generated from absorption of a photon in the absorber will reach the detectors via diffusion processes where they can be detected via tunneling. The absorption position and incident energy can be reconstructed using the different signals from the detectors adjacent to the absorber. The DROIDs described in this paper consist of Ta/Al STJs and a pure tantalum absorber. The lower energy gap of the proximized STJs will confine the quasiparticles under the tunnel barrier, thus improving the energy resolution and position sensitivity. With the DROID geometry described in this paper this confinement of the quasiparticles in the STJ is not perfect: to some extent quasiparticles can diffuse out of the STJs back into the absorber.

In this paper we describe an investigation of the effect of the last stage of the down conversion process in proximized STJs on the quasiparticle yield. In this regime the down conversion involves relaxation of high energy quasiparticles by phonon emission and breaking of Cooper pairs by energetic phonons providing additional quasiparticles. Using calculated phonon emission rates we simulate the final stages of the down conversion process in proximized tantalum/aluminum bilayers and compare the result with that of the hypothetic BCS counterpart with the same energy gap. To test the model we performed measurements of the ratio of charges from photon absorption in the proximized STJ and in the pure tantalum absorber immediately adjacent to the STJ of a DROID.

II. QUASIPARTICLE RELAXATION IN THE FINAL STAGE OF THE DOWN CONVERSION PROCESS

The quasiparticle density of states of a BCS-type superconductor, illustrated in Fig. 1(b), shows a singularity at the energy gap of the material and is constant throughout the layer thickness. Moving toward higher energy levels the quasiparticle density of states reduces asymptotically toward the value of $2N_0$ (the normal state single spins density of states) of the material.

In a proximized superconducting material, the quasiparticle density of states, the Cooper pair density, and the pair potential are all modified throughout the layers thickness. Brammertz *et al.*[13] noted that the pair potential displays a step at the interface and the energy gap (Δ_{s1+s2}) is constant throughout the complete structure, if the layer thickness is in the order of a few coherence lengths. The proximized quasiparticle density of states, illustrated in Fig. 1(a), is different in the two layers, varies across the thickness of the layers and is discontinuous at the interface. In the lower gap material (s_1) the quasiparticle density of states shows a broadened peak at the energy gap of the complete structure and in the higher gap material (s_2) a broadened peak is present at the energy gap of this material (Δ_{s2}) with a shoulder toward Δ_{s1+s2} creating the uniform energy gap throughout the two layers. Toward higher energies the density of states reduces asymptotically toward the value of $2N_0$ of the respective materials, identical to the BCS-type density of states.

The first two stages of the down conversion process occur at relatively high energies where the proximized structure and BCS-type structure appear identical and the down conversion will follow the same route. In the final stage of the down conversion the differences in quasiparticle density of states become more apparent. This stage is dominated by relatively slow relaxation of quasiparticles with release of a phonon. If $\hbar\Omega_{phonon}>2\Delta_{s1+s2}$, with $\hbar\Omega_{phonon}$ the energy of the released phonon, this phonon can break a Cooper pair releasing two more quasiparticles thus preserving the total energy. In contrast, subgap phonons ($\hbar\Omega_{phonon}<2\Delta_{s1+s2}$) cannot break Cooper pairs and the energy will be lost producing inefficiency in the energy preservation. This is accounted for by a factor of 1.75 (Ref. 14) in the expression for calculating the number of created quasiparticles following the absorption of a photon with energy E_0 in a BCS-type superconductor

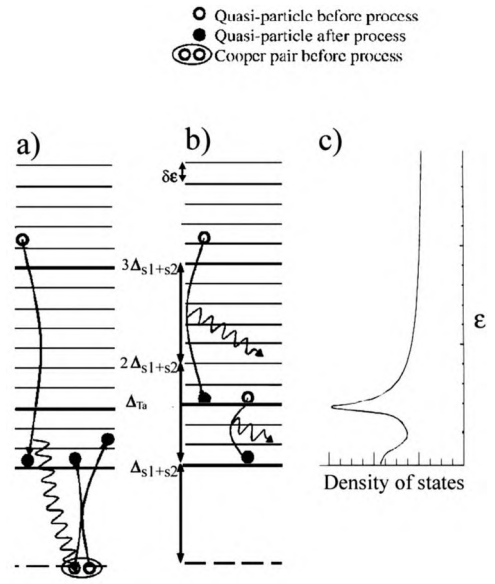

FIG. 2. The two routes of down conversion in a thin film proximized superconductor. (a) Relaxation of a quasiparticle to the energy gap producing two extra quasiparticles. (b) Relaxation of a quasiparticle toward the energy gap via the energy gap of the higher energy gap material producing no extra quasiparticles. (c) A schematic representation of the quasiparticle density of states of a proximized superconducting bilayer averaged over the bilayer thickness.

$$N = \frac{E_0}{1.75\Delta}, \tag{1}$$

with N as the number of quasiparticles and 1.75Δ as the average energy needed to break a Cooper pair.

The rate of spontaneous phonon emission is affected by the phonon density of states, which scales as Ω^2. An extra power of the initial energy of a quasiparticle enters because the number of final states below the initial energy ε_α is proportional to ε_α. On the other hand the quasiparticle relaxation is also dependent on density of electronic states. Since the quasiparticle density of states of a proximized superconductor is broadened and displays a maximum at Δ_{s2} in $s2$ this creates two possibilities. The first is emitting a high energy phonon and ending at an energy where the quasiparticle density of states is small [as in Fig. 2(a)] and the second is emitting a lower energy phonon and ending at an energy where the quasiparticle density of states is large [as in Fig. 2(b)]. In the process depicted in Fig. 2(a) relaxation from the initial state in the range $3\Delta_{s1+s2} \rightarrow 2\Delta_{s1+s2} + \Delta_{s2}$ can produce a productive phonon, $\hbar\Omega_{\text{phonon}} > 2\Delta_{s1+s2}$, which results in the breaking of a Cooper pair. In contrast, in the process in Fig. 2(b) where the energy of the emitted phonon is not sufficient, $\hbar\Omega_{\text{phonon}} < 2\Delta_{s1+s2}$, to generate extra quasiparticles and the system finally relaxes by emitting another nonproductive phonon.

III. PHONON EMISSION RATE IN BCS AND PROXIMIZED STRUCTURES

Comparison of the phonon emission rate for a proximized thin film superconductor with its BCS-type counterpart will indicate if the less efficient route is of importance for the quasiparticle yield. The local phonon emission rate Γ_{emi} is calculated using the following expression:[13,15]

$$\Gamma_{\text{emi}}(x, \varepsilon_\alpha \rightarrow \Delta\varepsilon_\beta) = \frac{1}{\tau_0(x)[kT_c(x)]^3} \int_{\varepsilon_\alpha - \varepsilon_\beta - \delta\varepsilon/2}^{\varepsilon_\alpha - \varepsilon_\beta + \delta\varepsilon/2} \Omega^2 \left[G(x, \varepsilon_\alpha - \Omega) - \frac{\Delta_1(x)}{\varepsilon_\alpha} \text{Im}\, F(x, \varepsilon_\alpha - \Omega) \right] [1 + n(\Omega)] d\Omega, \tag{2}$$

where x is the coordinate perpendicular to the interface between the two layers, ε_α and ε_β are the initial and final energies of the quasiparticle, τ_0 is the electron-phonon interaction characteristic time, T_c is the bulk critical temperature of the bilayer, both taken from literature.[16] Δ_1 is the position dependent order parameter, $G(x, \varepsilon)$ is the quasiparticle density of states, Im F is the imaginary part of the anomalous Green function, as explained in Ref. 13, and $n(\Omega)$ is the phonon distribution function which is in most cases smaller than unity and can be neglected. In the geometries discussed below the quasiparticles traverse the bilayer much faster than the time it takes to emit a phonon and the phonon emission rate can be averaged over the x-coordinate[17]

$$\Gamma_{\text{emi}}(\varepsilon_\alpha \rightarrow \varepsilon_\beta) = \frac{\int_{\text{electrode}} N_0(x) G(x, \varepsilon_\alpha) \Gamma_{\text{emi}}(x, \varepsilon_\alpha \rightarrow \varepsilon_\beta) dx}{\int_{\text{electrode}} N_0(x) G(x, \varepsilon_\alpha) dx}. \tag{3}$$

For the numerical evaluation of this expression, energy intervals of width $\delta\varepsilon$ (here chosen to be equal to $\Delta_{s1+s2}/11$) are used and the phonon emission rate from energy level ε_α to the energy interval $\delta\varepsilon_\beta$ near the energy ε_β can be averaged over the interval $[\varepsilon_\beta - \delta\varepsilon/2, \varepsilon_\beta + \delta\varepsilon/2]$

$$\Gamma_{\text{emi}}(\varepsilon_\alpha \rightarrow \delta\varepsilon_\beta) = \frac{\int_{\Delta\varepsilon_\alpha} \Gamma_{\text{emi}}(\varepsilon_\alpha \rightarrow \delta\varepsilon_\beta) d\varepsilon_\alpha}{\delta\varepsilon}. \tag{4}$$

From these expressions the phonon emission rate in the energy range Δ_{s1+s2} to $5\Delta_{s1+s2}$ has been calculated for a proximized Ta/Al superconducting thin film with thickness 100/60 nm (100 nm of tantalum and 60 nm of aluminum) and for the hypothetic BCS superconductor with the same energy gap ($\Delta_{s1+s2} = 420\ \mu$eV). The significance of the interval Δ_{s1+s2} to $5\Delta_{s1+s2}$ is that the maximum energy of the emitted phonons is less than $4\Delta_{s1+s2}$, hence there may only be one pair-breaking phonon emitted during the relaxation.

Figure 3 shows the calculated emission rate from any energy level ε_α, in the range of Δ to 5Δ, to any lower energy level ε_β. The BCS-type layers show the highest phonon emission rate, for all initial energies levels ε_α, to the final energy level $\varepsilon_\beta = \Delta_{s1+s2}$, while the proximized bilayer show the highest rate, for all initial energy levels ε_α, to the final energy level $\varepsilon_\beta = \Delta_{s2}$. This indicates that indeed quasiparticle creation in a proximized superconducting thin film proceeds with high efficiency through the route shown in Fig. 2(b).

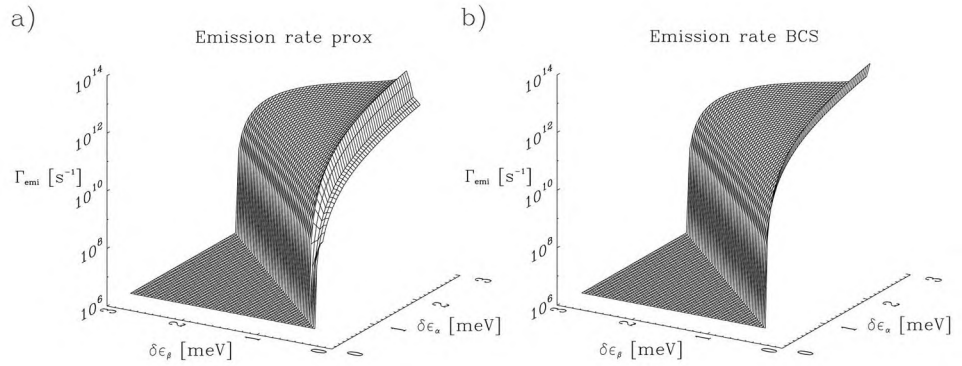

FIG. 3. The rate of phonon emission resulting from relaxations of a quasiparticle from energy ε_α to ε_β in the range of Δ to 5Δ (a) of a Ta/Al film 100/60 nm with an energy gap of 420 μeV and (b) of a BCS-type film with the same energy gap.

IV. QUASIPARTICLE CREATION EFFICIENCY

Using the phonon emission rate the final stage of down conversion can be modeled for the proximized and BCS-type superconductor thin films. The goal is to investigate if the efficiency of quasiparticle creation in a proximized structure is reduced in comparison with the efficiency of quasiparticle creation in a BCS structure with the same energy gap. For this comparison the number of quasiparticles created at the end of the down conversion process is of interest. The main reduction in the quasiparticle creation in a proximized superconductor will take place in the final relaxation toward the energy gap where the differences between the proximized and BCS density of states are the largest. This step is the relaxation from the range $3\Delta_{s1+s2} < \varepsilon < 5\Delta_{s1+s2}$ in which the phonons emitted due to relaxation can only break a single Cooper pair at most. Below this range the emitted phonons will not possess Cooper pair-breaking capabilities in either a proximized or a BCS-type superconductor thus not affecting the total number of quasiparticles. The energy dependent balance equation is given by[18]

$$\frac{dN(\delta\varepsilon_\alpha)}{dt} = \sum_\beta \Gamma_{\text{emi}}(\delta\varepsilon_\beta \rightarrow \delta\varepsilon_\alpha) \cdot N(\delta\varepsilon_\beta) - \sum_\beta \Gamma_{\text{emi}}(\delta\varepsilon_\alpha \rightarrow \delta\varepsilon_\beta) \cdot N(\delta\varepsilon_\alpha), \text{Equation} \quad (5)$$

with $N(\delta\varepsilon_\alpha)$ as the number of thermal quasiparticles in the energy interval $\delta\varepsilon_\alpha$. In order to account for quasiparticle creation due to breaking of Cooper pairs by high energetic phonons the number of emitted productive phonons ($\hbar\Omega \geq 2\Delta$) is of importance. When a phonon resulting from the relaxation from energy level ε_α to ε_β has Cooper pair-breaking capabilities it can produce two extra quasiparticles positioned at energy levels ε_γ and $\varepsilon_\alpha - \varepsilon_\beta - \varepsilon_\gamma$. A small amount of the productive phonons will be lost into the substrate before they can break a Cooper pair, but this is assumed to be negligible. As mentioned above only the total number of quasiparticles at the end of the down conversion process is of interest and not the dynamics of the quasiparticle distribution, which makes it possible to simplify the simulation of this process further. In the model each relaxation with $\varepsilon_\alpha - \varepsilon_\beta \geq 2\Delta$ is assumed to create two more quasiparticles, one of which is positioned at the energy gap and the other one is positioned at $\varepsilon_\alpha - \varepsilon_\beta - \Delta_{s1+s2}$. This simplification will produce a small error on the relaxation toward these energy levels because these levels will be more populated. However, in the required accuracy of the model this is negligible.

Using this model the final number of quasiparticles for different Ta/Al layouts has been calculated using the proximized and the BCS phonon emission rates. In this calculation we have used the density of states in Ta/Al bilayers as calculated with the model from Brammertz *et al.*[13] The energy gaps predicted for the experimentally tested structures in Sec. V were found in excellent agreement with the measured gaps. The density and energy gaps of the modeled geometries are only dependent on the layer thicknesses of the two materials. The rest of the parameters are the bulk values taken from literature.[16] The ratio of numbers of calculated created quasiparticles in the proximized structure and in the BCS counterpart ($N_{\text{prox}}/N_{\text{BCS}}$) for the different geometries is shown as a function of tantalum layer thicknesses for three different aluminum thicknesses in Fig. 4. In all cases the ratio $N_{\text{prox}}/N_{\text{BCS}}$ is smaller than unity indicating that the calculated quasiparticle creation is indeed less efficient in proximized structures.

For tantalum thicknesses larger than a few coherence lengths ($x_0 \sim 90$ nm) the proximized quasiparticle density of states will approach the quasiparticle density of states of pure tantalum and display a sharp peak near the energy gap of tantalum. In the proximized part of the structure the energy gap Δ_{s1+s2} will be constant with tantalum thickness, in the nonproximized tantalum the energy gap will be equal to Δ_{Ta}(=700 μeV) and in between there will be a intermediate region where the energy gap changes from Δ_{s1+s2} to Δ_{Ta}. The effect of the proximized density of states will reduce with increasing tantalum thickness and the device will appear

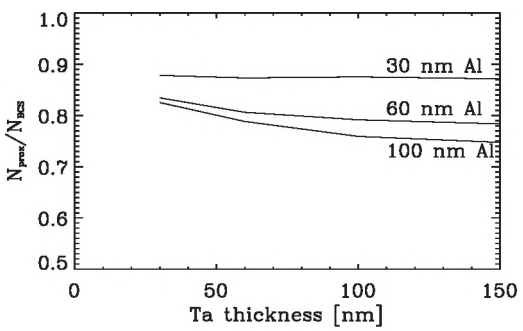

FIG. 4. Ratio of quasiparticle yield in a proximized Ta/Al bilayer and in the BCS counterpart as a function of tantalum layer thickness for aluminum thicknesses 30, 60, and 100 nm.

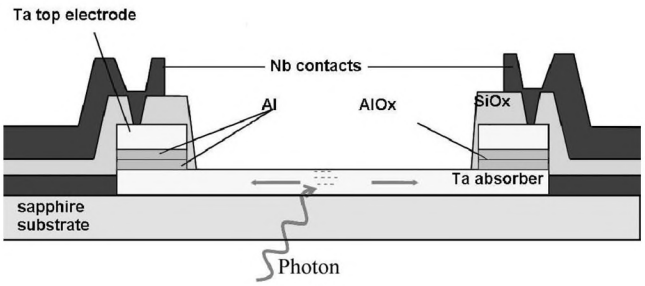

FIG. 5. Schematic representation of the DROID configuration.

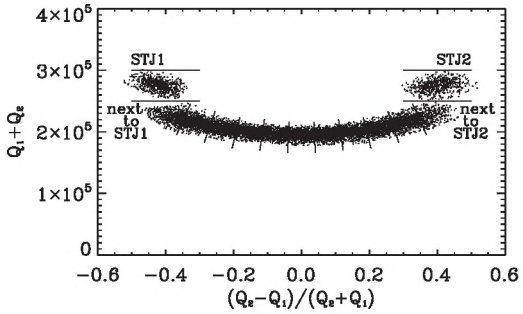

FIG. 6. Scatter plot of the total charge output, measuring a photon energy, against the ratio of the charges, measuring the position of absorption site, for the 100/30 nm Ta/Al DROID and a wavelength of 300 nm. The lines show a graphical representation of the selection of the different areas with the sections used to calculate the ratios indicated.

more like BCS tantalum with the ratio $N_{\mathrm{prox}}/N_{\mathrm{BCS}}$ approaching $\Delta_{s1+s2}/\Delta_{\mathrm{Ta}}$ (0.71, 0.60, and 0.51 for Al thicknesses of 30, 60, and 100 nm, respectively).

Due to the finite bin size $\delta\varepsilon$ in the numerical calculation of the averaged phonon emission rate [Eq. (4)], the number of states in the sharp peak at Δ_{Ta} for thick Ta layers tends to get underestimated, and hence also the contribution of the relaxation through this channel. The efficiency of quasiparticle creation will be overestimated and the calculated ratio $N_{\mathrm{prox}}/N_{\mathrm{BCS}}$ for thicker tantalum layer will be too large. For this reason we only display calculations for layer thicknesses up to a few coherence lengths. Note that the BCS quasiparticle density of states shows a similar sharp peak near the energy gap. However, in this case underestimation of the number of states in the peak has only a minor effect, since there is only a single relaxation channel.

V. EXPERIMENTAL INVESTIGATION OF THE QUASIPARTICLE YIELD IN THE BCS ABSORBER AND PROXIMIZED STJ OF A DROID

To test the model we compared the charge outputs (defined as the number of tunneled electrons) of photon absorption events occurring inside an STJ with those in the absorber immediately next to the STJ, in three DROID structures with different STJ layer structures. Within a DROID we can measure the charge output (e^-) of a proximized superconductor (the STJ) and a BCS-type superconductor (the absorber) within a single experiment. Since the two types of superconductor are part of the same detector the measurement parameters such as film quality, operating temperature, and magnetic field are identical. The DROIDs, produced by MicroFab Ltd (Ref. 19) using high quality sputter targets (purity of 99.99%) and *r*-plane Sapphire substrates, have a length, including the STJs, of 400 μm and a width of 30 μm. The STJs are square in geometry with the sides equal to the width of the absorber. The tantalum layer of the base electrode of the STJ is an integral part of the pure BCS tantalum absorber (see Fig. 5) which has an energy gap of 700 μeV. The STJs are made out of a Ta/Al/AlO_x/Al/Ta multilayer with thicknesses of 100/30/1/30/100 nm, 100/60/1/60/100 nm, and 100/100/1/100/100 nm energy gaps, as measured from the IV curves of 500, 420, and 360 μeV and residual resistivity ratio values of 50, 59, and 41, respectively. The confinement of the quasiparticles in the STJ improves with aluminum layer thickness due to the lower energy gap. For the 100 nm aluminum layer the confinement is nearly perfect which means that the quasiparticles cannot escape from the STJ.

A ^{3}He sorption cooler has been used with a base temperature of 295 mK, low enough to reduce the thermal current to a negligible level for all three devices. The cryostat is equipped with an optical fiber to illuminate the chip through the sapphire substrate with optical photons (E_0=1–5 eV) from a double grating monochromator.

The signal pulses from the STJs are fed into a charge sensitive preamplifier and subsequently digitized in a computer oscilloscope card. In a DROID structure the generated quasiparticles will diffuse throughout the structure and are detected by tunneling across the barrier in the STJs. The sum of the measured charge outputs Q_1+Q_2 is a measure of the photon energy, while the normalized difference $(Q_1-Q_2)/(Q_1+Q_2)$ refers to position of absorption along the absorber. Figure 6 shows a scatter plot of individual photon signals in an energy versus position representation. Absorptions in the STJs can easily be distinguished from those in the absorber by their spatial separation. The pulses from a single position are averaged to reduce the noise and integrated to obtain the charge output. To ensure that the detected quasiparticles undergo the same loss due to diffusion the STJ charge output is compared to the charge output of an area on the absorber next to the STJ. This area should be sufficiently large so that the lateral proximity effect[20] has a negligible influence. Also it should not be big enough for the differences in loss due to diffusion through the absorber to become apparent. An area with a width of 33 μm is chosen, which divides the absorber in 11 sections (see Fig. 6). This is much larger than the extent of the lateral proximity effect, which is only for a few micrometers, and it is well within the position resolution of the devices used.

There are some differences between an absorption in the STJ and one in the absorber which have to be taken into consideration. For photon absorption in the STJ the quasiparticles will ultimately relax toward Δ_{STJ}. Quasiparticles which are generated due to absorption in the absorber will ultimately relax toward Δ_{Ta} and diffuse toward the STJs where they are injected into the STJ at Δ_{Ta}. The relaxation time of these quasiparticles is much faster than the time required for diffusing into and out of the STJ and the quasiparticles will relax with emission of a phonon.

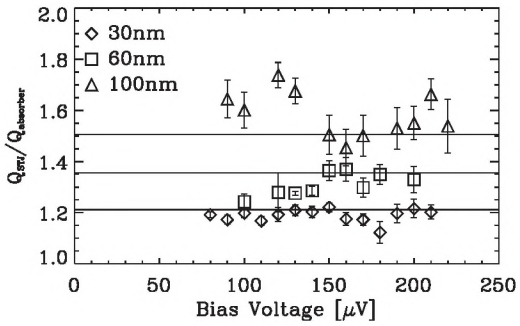

FIG. 7. Ratio of the charge output of absorption in the STJ and in the absorber right next to the STJ for the three layouts at different bias voltages. The three lines are the calculated ratios.

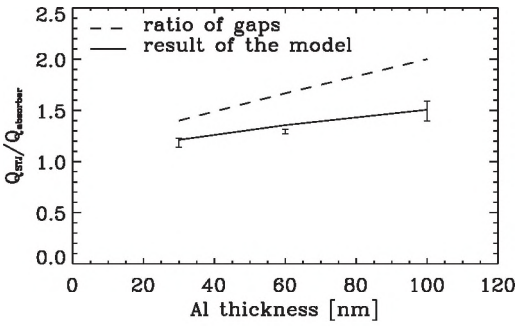

FIG. 8. Ratio of the charge output from the STJ and from the absorber just next to the STJ for the DROIDs with aluminum layer thickness of 30, 60, and 100 nm, all with a tantalum layer thickness of 100 nm. The dashed line is the predicted ratio for a BCS-type STJ with energy gap Δ_{STJ}. The solid line is the ratio as calculated obtained with the model. The presented points are averages of the measured ratios at different photon energies in the range of 1.5–5 eV over which range the ratio is constant in all three cases. The ratios for the bilayers with 30 nm aluminum have been measured at a bias voltage of 100 μV and the ratios for the bilayers with 60 and 100 nm aluminum have been measured at 150 μV.

Under the influence of gain in energy due to sequential tunneling, relaxation with emission of a phonon and the in- and out-flux of quasiparticles between the STJ and absorber a quasistationary spectral distribution of quasiparticles will be formed in both situations. This quasiparticle distribution will retain its spectral shape during the whole process of charge acquisition, while the number of nonequilibrium quasiparticles (area under the spectral distribution curve) decreases as quasiparticles are lost or recombine. The effect of the different initial conditions in distribution between absorption in the STJ and that in the absorber on the shape of the spectral distribution is expected to be negligible. However, the confinement of quasiparticles in the STJ could have an effect on the charge output ratio, e.g., with perfect confinement all quasiparticles generated resulting from an absorption in the STJ would remain in the STJ. While for an absorption in the absorber a fraction of the quasiparticles would diffuse toward the opposite STJ, experiencing the loss mechanisms in the absorber. The confinement of quasiparticles is affected by the applied bias voltage. With each tunnel event a quasiparticle gains energy equal to the bias voltage, this is counteracted by relaxation, and with increasing bias voltage the confinement will reduce. If the confinement has an effect on the ratio of charges in the way explained above it should be visible in a scan over different bias voltages. Because with reduced confinement in the STJ the quasiparticles created in the STJ will be subjected to more losses (the losses in the absorber) the ratio Q_{STJ}/Q_{abs} should reduce with bias voltage. Figure 7 shows the ratio of the measured charge outputs for photon absorption in the STJ and for absorption in the absorber next to the STJ as a function of bias voltage. Even if the data of the thicker aluminum devices show a lot of scatter due to noise, no trend is visible in all three situations and we conclude that the extra losses for quasiparticles produced by an absorption in the absorber immediately adjacent to the STJ are negligible.

In the model the multiple tunneling is seen as an amplification of the number of generated quasiparticles which is the same for absorption in the STJ and for absorption in the absorber. Thus in both situations the charge output is a measure of the number of quasiparticles generated and the ratio should be equal to the ratio of the number of created quasiparticles following the absorption of a photon on each position.

If the proximized STJs were acting like BCS-type STJs the ratio between the charge output in the STJ and the absorber section next to the STJ would simply be determined by the ratio of the energy gaps [cf. Eq. (1)].

$$\frac{Q_{STJ,BCS}}{Q_{abs}} = \frac{\Delta_{Ta}}{\Delta_{STJ}}. \tag{6}$$

Here $Q_{STJ,BCS}$ is the charge output of a BCS-type STJ and Q_{abs} is the charge output of the absorber. However, taking into account the lower quasiparticle yield in the proximized STJ we arrive at a lower ratio.

$$\frac{Q_{STJ,prox}}{Q_{abs}} = \frac{\Delta_{Ta}}{\Delta_{STJ}} \frac{N_{prox}}{N_{BCS}}. \tag{7}$$

Here $Q_{STJ,prox}$ is the charge output of the proximized STJ and N_{prox}/N_{BCS} is the calculated ratio of the numbers of created quasiparticles for a proximized and for a BCS-type density of states for the STJ, which can be calculated using the model explained in Sec. IV. From Eq. (7) the ratio $Q_{STJ,prox}/Q_{abs}$ has been calculated for DROIDs with 30, 60, and 100 nm thick aluminum layers in the STJs. The results are compared with the ratio of the charge output of the STJ and the part of the absorber immediately next to the STJ for different photon energies ranging from 1.5 to 5 eV for the different devices. The bias voltage was 100 μV for the DROID with 30 nm aluminum layers and 150 μV for the DROIDs with 60 and 100 nm aluminum layers. For all three aluminum thicknesses the ratio is constant with photon energy and the ratios of a single energy scan have been averaged to increase the accuracy. The results are shown in Fig. 8 where the points are the measured ratios, the dashed line is the ratio Δ_{Ta}/Δ_{STJ} and the solid line is the resulting ratio of the model.

For all three DROIDs the measured ratios are well below the ratio Δ_{Ta}/Δ_{STJ} indicating the significance of different conditions for the quasiparticle creation. The simulated ratio convincingly fits the results in all three measurements.

VI. DISCUSSION

We have investigated the final stage of down conversion in proximized thin film superconductors and clearly confirmed a lower efficiency in quasiparticle creation compared to the BCS counterpart. This lower efficiency is caused by the modified quasiparticle density of states of a proximized device (shown in Fig. 1) which, contrary to the BCS quasiparticle density of states shows an increased number of states at Δ_{s2} in the higher gap material. In the final stage of the down conversion process of a proximized superconducting thin film, the result will be an increase in relaxation of high energy quasiparticles first toward Δ_{s2} followed by relaxation toward Δ_{s1+s2}, instead of immediately relaxing toward Δ_{s1+s2} as in a BCS-type superconductor. Quasiparticles from the energy range $3\Delta_{s1}$ to $2\Delta_{s1+s2}+\Delta_{s2}$ which relax to Δ_{s2} do not emit phonons with Cooper pair-breaking capabilities while the phonons would be energetic enough to break a Cooper pair if the quasiparticle immediately would have relaxed to Δ_{s1+s2}. This results in reduced quasiparticle creation efficiency in proximized superconducting thin films.

The reduced quasiparticle creation efficiency is confirmed in the measurements using DROIDs where we have compared the charge output of the proximized STJ with the charge output of the BCS absorber. Figure 8 clearly shows that the ratio of the two responsivities is lower than the ratio of the energy gaps. Using the model we have calculated the ratio as it would be with the lower efficiency in quasiparticle creation in the proximized STJ. In all three situations the calculated ratio closely fits the measured ratios. For the measurements it is assumed that the difference in loss of quasiparticles due to diffusion is negligible for these two locations. Although the quasiparticle diffusion and injection in the STJ are different for the two locations a constant distribution of quasiparticles is quickly formed, which is the same in shape but different in amplitude. The trapping of quasiparticles in the STJ could produce a lower loss rate for quasiparticles created in the STJ. However, a variation in the bias voltage, which changes the trapping efficiency of the STJs, has no effect on the ratio indicating this effect is negligible. The ratio of the responsivities is constant with photon energy in the optical range. With the absorption of an optical photon the quasiparticle concentration is too low to produce significant recombination between two mobile quasiparticles, which would reduce the charge output in both the STJ and absorber. Also the number of states available in the quasiparticle density of states is large enough to accommodate all generated quasiparticles close to the edge of the energy gap, such that no restriction in the relaxation of quasiparticles is introduced.

For photon detectors based on proximized superconductors, such as STJs, the implication of this lower quasiparticle yield at the end of the down conversion is lower signal amplitude and a lower limiting energy resolving power. In the case of a DROID, where the absorber is made of a pure superconductor and the STJs are proximized superconductors, the charge output of the STJ will be lower than one would assume from the ratio of the energy gaps of the STJ and absorber. Also the resolution of the STJs will be affected accordingly.

VII. CONCLUSION

In conclusion we have successfully clarified in significant detail the final stages of down conversion in proximized superconducting thin films and compared them to the BCS counterpart with the same energy gap. The model has been tested using the ratio of the charge output of the proximized STJ and BCS-type absorber of three DROIDs with different aluminum trapping layer thicknesses in the proximized STJs. The experimental data agree closely with the model. We conclude that the quasiparticle creation in proximized devices compared with a BCS-type superconductor is indeed less efficient due to increased quasiparticle relaxation toward the energy gap of the higher gap material.

ACKNOWLEDGMENTS

We would like to thank Dr. A.A. Golubov from the Department of Applied Physics, University of Twente, Enschede, the Netherlands for the useful discussions.

[1]K. D. Irwin, Appl. Phys. Lett. **66**, 1998 (1995).
[2]P. Day, H. Leduc, B. Mazin, A. Vayonakis, and J. Zmuidzinas, Nature (London) **425**, 817 (2003).
[3]A. Peacock, P. Verhoeve, N. Rando, A. van Dordrecht, B. G. Taylor, C. Erd, M. A. C. Perryman, R. Venn, J. Howlett, D. J. Goldie, J. Lumley, and M. Wallis, Nature (London) **381**, 135 (1996).
[4]D. Van Vechten and K. Wood, Phys. Rev. B **43**, 12852 (1991).
[5]Yu. N. Ovchinnikov and V. Z. Kresin, Phys. Rev. B **58**, 12416 (1998).
[6]A. G. Kozorezov, A. F. Volkov, J. K. Wigmore, A. Peacock, A. Poelaert, and R. den Hartog, Phys. Rev. B, **61**, 11807 (2000).
[7]J. Bardeen, L. N. Cooper, and J. R. Schrieffer, Phys. Rev. **108**, 1175 (1957).
[8]A. G. Kozorezov, J. K. Wigmore, A. Peacock, A. Poelaert, P. Verhoeve, R. den Hartog, and G. Brammertz, Appl. Phys. Lett. **78**, 3654 (2001).
[9]R. Barends, J. J. Baselmans, S. J. C. Yates, J. R. Gao, J. N. Hovenier, and T. M. Klapwijk, Phys. Rev. Lett. **100**, 257002 (2008).
[10]A. V. Timofeev, C. Pascual Garcia, N. B. Kopnin, A. M. Savin, M. Maschke, F. Giazotto, and J. P. Pekola, Phys. Rev. Lett. **102**, 017003 (2009).
[11]N. E. Booth, Appl. Phys. Lett. **50**, 293 (1987).
[12]H. Kraus, F. v. Feilitzsch, J. Jochum, R. L. Mössbauer, Th. Peterreins, and F. Pröbst, Phys. Lett. B **231**, 195 (1989).
[13]G. Brammertz, A. Poelaert, A. A. Golubov, P. Verhoeve, A. Peacock, and H. Rogalla, J. Appl. Phys. **90**, 355 (2001).
[14]M. Kurakado, Nucl. Instrum. Methods Phys. Res. **196**, 275 (1982).
[15]A. A. Golubov, E. P. Houwman, J. G. Gijsbertsen, J. Flokstra, and H. Rogalla, Phys. Rev. B **49**, 12953 (1994).
[16]S. B. Kaplan, C. C. Chi, D. N. Langenberg, J. J. Chang, S. Jafarey, and D. J. Scalapino, Phys. Rev. B **14**, 4854 (1976).
[17]B. A. Aminov, A. A. Golubov, and M. Yu. Kupriyanov, Phys. Rev. B **53**, 365 (1996).
[18]A. G. Kozorezov, R. A. Hijmering, G. Brammertz, J. K. Wigmore, A. Peacock, D. Martin, P. Verhoeve, A. A. Golubov, and H. Rogalla, Phys. Rev. B **77**, 014501 (2008).
[19]D. D. E. Martin, Ph.D. thesis, University of Twente, Enschede, 2007.
[20]R. den Hartog, A. A. Golubov, P. Verhoeve, A. Poelaert, D. Martin, A. Peacock, A. van Dordrecht, and D. J. Goldie, Phys. Rev. B **63**, 214507 (2001).